A Bilateral In Vitro Model for Cardiovascular Disease Investigations Using Photoplethysmography Sensors

Redjan Ferizoli, Parmis Karimpour, James M. May, *Member IEEE* & Panayiotis A. Kyriacou, *Senior Member IEEE*
Research Centre for Biomedical Engineering, City, University of London, UK, EC1V 0HB
Email: Redjan.Ferizoli@city.ac.uk

***Abstract*—Photoplethysmography (PPG) is a noninvasive optical sensing technique utilised widely for the assessment of cardiovascular disease (CVD). As CVD is the leading cause of mortality globally, there is a significant interest in the innovation of new and robust noninvasive technologies for the early detection of CVD. This work aimed to develop and evaluate vascular tissue phantoms using the techniques of PPG. The paper describes the fabrication process of custom vessels and the formation of tissue phantoms. In addition, PPG measurement protocols utilising the developed tissue phantoms in an in vitro cardiovascular flow rig were also employed. Following analysis of the acquired PPGs, including feature extraction and statistical analysis, the results demonstrated for the first time that PPGs can be successfully acquired from two identical tissue phantoms placed in a bilateral configuration. This research paves the way for investigating PPGs in a controlled in vitro environment including examining the effect of vascular ageing (arterial stiffness) on the PPG signals.**

Keywords—photoplethysmography; cardiovascular disease; optical sensors

I. Introduction

Approximately 17.9 million deaths occurred in 2019 due to cardiovascular diseases (CVD), making it the leading cause of death globally [1]. The established optical sensing technique of photoplethysmography (PPG), has a huge potential for cardiovascular health assessment [2]. PPG is commonly used for the estimation of blood oxygen saturation and heart rate in the well-established technique of pulse oximetry, and for the measurement of pulse (heart) rate in most wearable devices [3]. For many years research has suggested that the PPG relates to changes in cardiovascular health [4]. Of particular interest in this research is the relation of PPG with vascular ageing, where in such cases stiffening of the arteries alters the structure and haemodynamics of blood flow, leading to CVD [5]. This paper proposes that PPG can be used as a primary technique to investigate the vascular system, whereby a PPG signal can alter depending on the properties of different vessels.

PPG employs light to non-invasively measure volumetric changes in blood vessels [6]. Devices which incorporate PPG-based sensors can be placed on various body sites, such as the fingertip, wrist, forehead, foot, and ears. The main two components of a PPG sensor are the light source(s), typically LEDs, and photodetectors such as photodiodes or phototransistors. The light source illuminates the tissue at the body site, and the light received by the photodetector is measured [7]. As the heart cycles through the systolic and diastolic phases, the variations in blood volume are represented as the photoplethysmograph [8].

PPG has become widely used in consumer wearables due to its simplicity and relatively low cost. Continuous measurements are possible with most PPG-based devices since only a single contact point is required to obtain measurements [9]. Yet, it is also possible to record PPG simultaneously across multiple sites. Prior research has demonstrated that coronary artery disease, peripheral arterial disease, and ageing may all be evaluated using multi-site PPG [10]–[13].

II. Method

A. Fabricating Custom Vessels

Using an experimental setup, commercial tubing was coated with a silicone layer to create customised vessels. The procedure involves using PlatSil Gel-10 (Polytek Development Corp., Easton, PA). The product has two parts: Part A and Part B. Care was taken to avoid contamination across the parts to prevent premature curing. Equal amounts of Part A and Part B were poured into a mixing container. To extend the pour time to help ensure uniform coating and a regular wall thickness along the length of the custom tube, PlatSil 71/73 Retarder (Polytek Development Corp., Easton, PA) was added at a rate of 1.5 % of the total weight. Each elastomer mixture contained 40.6 g of total material in weight. Following the technical bulletin, adding 1 % retarder to the total weight increases the working time from 6 minutes to 12 minutes [14]. The mixture was blended and placed into a vacuum chamber, which removed the air bubbles, and then poured into the silicone pot ready for the dip coating stage.

The dip coating technique followed the procedure developed by Nomoni et al. [15], set up as shown in Fig. 1. Commercial silicone tubing was attached to the pulleys and passed through the heating element. A tension weight was attached to one side of the commercial tubing whilst the other side was attached to the dip coater arm. To help cure the coating layer, the heating element was increased to 275 C. The commercial tubing was pulled up at a speed of 40 mm/s to add a coating layer using the elastomer mixture. Once the arm reached the maximum height, the dip coated tubing was left to cure. Once cured, the internal commercial tubing was carefully removed, separating it from the custom vessel.

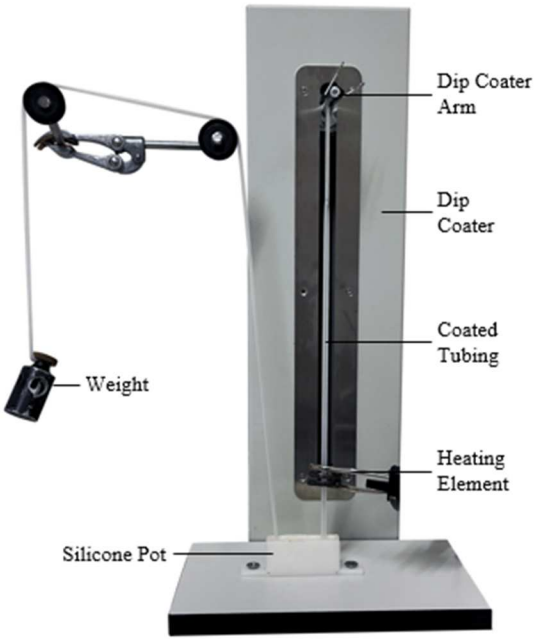

Fig. 1. Dip-coating setup for producing silicone vessels. Commercial tubing is pulled through a silicone pot to become coated in the silicone mixture, followed by a heating element to accelerate the curing of the silicone coating. Finally, the inner tubing is removed, leaving the silicone coating as a custom vessel.

B. Forming Tissue Phantoms

The tissue phantoms were made following a procedure similar to the custom vessel construction. Equal amounts of Part A and Part B of Gel-10 were mixed with retarder to increase the working time. Additionally, Smiths Deadener (Polytek Development Corp., Easton, PA) was mixed to create softer tissue of OO30 shore hardness, measured using an AD-100-OO Precision Shore Durometer (Checkline Europe, Netherlands), in line with a reported porcine tissue hardness [16]. The ratio of the components was 1A:1B:1.75D. Once the materials were mixed, the container was placed into the vacuum chamber to remove air bubbles. Then, the mixture was poured into 3D-printed moulds and left to cure. The cured tissue phantoms were attached to the bilateral model.

C. Bilateral In Vitro Model

The experimental setup consisted of multiple components simulating the cardiovascular system. The vascular system was built around a pulsatile pump (Model 1423 PBP, Harvard Apparatus, US) which simulated the human heartbeat and produced pulsatile flow with a realistic PPG wave.

The vascular system surrounding the phantoms was built with clear silicone rubber tubing (Hilltop Products, UK). Thin-walled tubing of less than 1 mm was used; ensuring high elasticity to mimic human arteries. This enhanced the presence of a dicrotic notch in the PPG signal. Various sizes of tubing were joined together using custom 3D-printed connectors, designed in Fusion 360 (Autodesk, US), and printed with the Saturn 3D Resin Printer (Elegoo, China) using standard photopolymer resin. This enabled the use of in-line pressure sensors with luer connections, customised diameters, and custom connection types such as curved, angled, and Y-connectors.

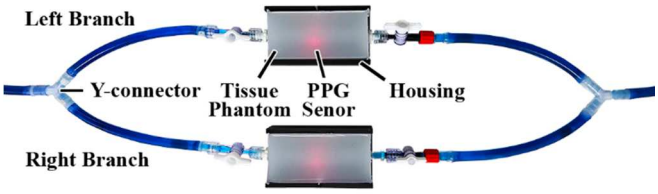

Fig. 2. Bilateral phantoms, consisting of custom vessels surrounded by tissue, situated inside 3D-printed housing featuring PPG sensors for simultaneous measurement.

To create a simple blood mimicking fluid (BMF), deionised water was mixed with methylene blue powder (Thermo Fisher Scientific, UK). This increased the amount of light absorbed at the red and infrared (IR) wavelengths. The peak absorption of methylene blue is in the red region, between 650 nm and 700 nm [17]. An advantage of methylene blue was the simple procedure for mixing. To introduce this fluid into the system, a raised reservoir was placed above the setup, adding gravitational pressure.

As aforementioned, the vessel-tissue phantoms were connected to the vascular setup via a bifurcation, introduced with a y-connector to simultaneously record PPG signals from each phantom, shown in Fig. 2. The phantoms were placed in 3D-printed retainers which housed a custom-built PPG sensor, consisting of red and IR LEDs (peak absorption wavelengths 640 nm and 900 nm, respectively) and a photodiode (900 nm peak sensitivity) (BPW34, Osram Germany). The sensors were connected to the ZenPPG, a custom-made dual-channel device for PPG signal acquisition and processing, developed in the Research Centre for Biomedical Engineering at City, University of London [18].

III. Results & Discussion

PPG signals from each branch were filtered and displayed using MATLAB (The MathWorks, USA). Both phantoms produced visually similar PPG signals, as seen in Fig. 3. This indicated that the two branches of the system had similar flow profiles and light-tissue interaction properties. Noise is present at the systolic peak, possibly due to mechanical vibrations in the system, which may be mitigated by using a non-mechanical pump.

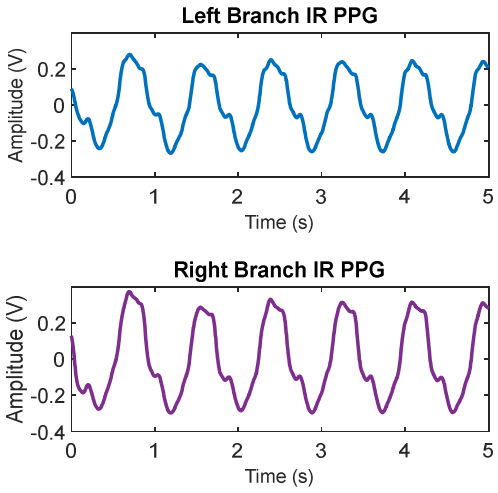

Fig. 3. Infrared PPG signals from both branches of the bilateral in vitro setup.

PPG feature extraction was conducted to validate and quantify the similarity of the two signals. A custom Python algorithm developed at City, University of London was used. [19]. This produced morphological features of the PPG waves based on the systolic peaks and the troughs of the signal, measured geometrically. The *amplitude* of the peak, gradients of the *upslope, downslope*, and time taken for the wave to *rise* and *decay* were calculated.

Statistical analysis of the resultant features was employed to determine the degree of conformity between the PPG signals from the two branches. Each PPG feature was analysed for statistical significance, using the Kruskal-Wallis one-way analysis of variance. By feeding in the list the values for each feature, this method tested the hypothesis that the samples have been drawn from the same population. As this experiment involved phantoms from the same silicone mixture, the hypothesis was that differences between the samples would be statistically insignificant.

For each PPG feature, the Kruskal-Wallis analysis provided a p-value, showing the statistical similarity between the two branches. The range of values for the features are presented in the box plots shown in Fig. 4. The distribution shows that both branches produced morphologically similar PPG signals. Amplitude, downslope, rise time and decay time were statistically similar ($p > 0.05$), indicating that these features were from the same distribution. This result confirmed that the bilateral setup consisted of identical phantoms, which can be used for further PPG experiments in CVD.

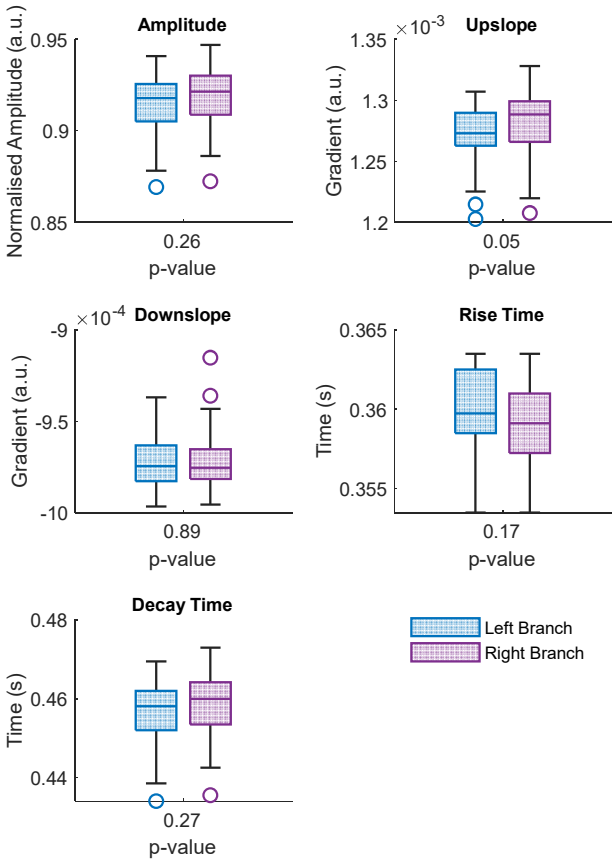

Fig. 4. Kruskal-Wallis analysis of infrared PPG features from the two phantoms, comparing their similarity for each feature (a.u. = arbitrary unit). P > 0.05 indicates that the phantoms are statistically identical.

This experiment was repeated to validate the findings. Table I presents the p-values obtained from the statistical analysis of each experiment. These results showed a similar pattern; the p-values for amplitude, downslope, and decay time indicated statistical similarity. Variations were present when comparing the same wavelengths across different experiments, however, the p-values were typically above the threshold for statistical significance ($p > 0.05$). The differences between experiments could be due to changes in the measuring environment, such as temperature and ambient lighting. Rise time did show a statistical difference, with most of the p-values below 0.05. However, this was less common in the IR signals, suggesting that IR PPG signals are more stable. The overall similarity between the two branches, across multiple experiments, establishes a route for the use of bilateral in vitro models in CVD studies

TABLE I. P-VALUES OF RED AND INFRARED (IR) PPG FEATURES

	Experiment 1		**Experiment 2**		**Experiment 3**	
Feature	***Red***	***IR***	***Red***	***IR***	***Red***	***IR***
Amplitude	0.84	0.26	0.45	0.68	0.57	0.96
Upslope	0.38	0.05	0.55	0.08	0.53	0.20
Downslope	0.57	0.89	0.53	0.56	0.71	0.02
Rise Time	0.02	0.17	0.03	0.01	0.03	0.18
Decay Time	0.78	0.27	0.45	0.72	0.56	0.95

P > 0.05 indicates that the two phantoms are statistically identical.

IV. CONCLUSION

PPG is a valuable optical sensing technology with recent advancements showing potential for CVD assessment. This study proposed using PPG for such investigations, particularly in vascular health, by developing and testing a bilateral in vitro flow rig.

The method involved fabricating custom vessels and forming tissue phantoms, which were connected to the cardiovascular flow test model for simultaneous PPG signal acquisition. Customised algorithms were used to extract morphological features from the resultant signals and analysed for statistical similarity. Statistical outcomes validated that PPG signals generated in a bilateral vessel-tissue phantom configuration were largely identical, indicating their potential use in CVD investigations.

Future phantoms can be altered to mimic aged or diseased vessels by varying the ratio of elastomers to modify the stiffness properties. Enhancements of the in vitro rig would allow for more precise feature extraction and better detection of variations during CVD. This could be achieved by reducing mechanical vibrations to improve signal quality and implementing one-way valves to prevent cross-flow.

This research facilitates further in vitro experiments involving bilateral phantoms where pathologies such as arterial stiffness and atherosclerosis can be deliberately introduced, through which PPG signals can be compared and therefore new sensors designed to help improve CVD assessment.

REFERENCES

[1] D. T. Lackland and M. A. Weber, 'Global burden of cardiovascular disease and stroke: hypertension at the core', *Can J Cardiol*, vol. 31, no. 5, pp. 569–571, May 2015, doi: 10.1016/j.cjca.2015.01.009.

[2] J. Park, H. S. Seok, S.-S. Kim, and H. Shin, 'Photoplethysmogram analysis and applications: an integrative review', *Frontiers in Physiology*, vol. 12, 2022, Accessed: Sep. 04, 2022. [Online]. Available: https://www.frontiersin.org/articles/10.3389/fphys.2021.808451

[3] T. Tamura, 'Current progress of photoplethysmography and SPO2 for health monitoring', *Biomed. Eng. Lett.*, vol. 9, no. 1, pp. 21–36, Feb. 2019, doi: 10.1007/s13534-019-00097-w.

[4] A. S. Al Fahoum, A. O. Abu Al-Haija, and H. A. Alshraideh, 'Identification of coronary artery diseases using photoplethysmography signals and practical feature selection process', *Bioengineering (Basel)*, vol. 10, no. 2, p. 249, Feb. 2023, doi: 10.3390/bioengineering10020249.

[5] M. Sawabe, 'Vascular aging: from molecular mechanism to clinical significance', *Geriatrics & Gerontology International*, vol. 10, no. s1, pp. S213–S220, 2010, doi: 10.1111/j.1447-0594.2010.00603.x.

[6] M. Elgendi *et al.*, 'The use of photoplethysmography for assessing hypertension', *npj Digit. Med.*, vol. 2, no. 1, Art. no. 1, Jun. 2019, doi: 10.1038/s41746-019-0136-7.

[7] D. Castaneda, A. Esparza, M. Ghamari, C. Soltanpur, and H. Nazeran, 'A review on wearable photoplethysmography sensors and their potential future applications in health care', *Int J Biosens Bioelectron*, vol. 4, no. 4, pp. 195–202, 2018, doi: 10.15406/ijbsbe.2018.04.00125.

[8] S. Nara, M. Kaur, and K. Lal Verma, 'Novel notch detection algorithm for detection of dicrotic notch in ppg signals', *IJCA*, vol. 86, no. 17, pp. 36–39, Jan. 2014, doi: 10.5120/15081-3520.

[9] Y. Sun and N. Thakor, 'Photoplethysmography revisited: from contact to noncontact, from point to imaging', *IEEE Transactions on Biomedical Engineering*, vol. 63, no. 3, pp. 463–477, Mar. 2016, doi: 10.1109/TBME.2015.2476337.

[10] G. Chan *et al.*, 'Multi-site photoplethysmography technology for blood pressure assessment: challenges and recommendations', *J Clin Med*, vol. 8, no. 11, p. 1827, Nov. 2019, doi: 10.3390/jcm8111827.

[11] J. Allen, J. O'Sullivan, G. Stansby, and A. Murray, 'Age-related changes in pulse risetime measured by multi-site photoplethysmography', *Physiol. Meas.*, vol. 41, no. 7, p. 074001, Jul. 2020, doi: 10.1088/1361-6579/ab9b67.

[12] M. Bentham, G. Stansby, and J. Allen, 'Innovative multi-site photoplethysmography analysis for quantifying pulse amplitude and timing variability characteristics in peripheral arterial disease', *Diseases*, vol. 6, no. 3, p. 81, Sep. 2018, doi: 10.3390/diseases6030081.

[13] V. Ouyang *et al.*, 'The use of multi-site photoplethysmography (PPG) as a screening tool for coronary arterial disease and atherosclerosis', *Physiol. Meas.*, vol. 42, no. 6, p. 064006, Jun. 2021, doi: 10.1088/1361-6579/abad48.

[14] 'Polytek_TB_PlatSilGels_5-5-2021.pdf'. Accessed: Jan. 25, 2023. [Online]. Available: https://polytek.com/content/pdf/technicalbulletin/Polytek_TB_PlatSilGels_5-5-2021.pdf

[15] M. Nomoni, J. M. May, and P. A. Kyriacou, 'Fabricating novel PDMS vessels for phantoms in photoplethysmography investigations.', *Annu Int Conf IEEE Eng Med Biol Soc*, vol. 2020, pp. 4458–4461, Jul. 2020, doi: 10.1109/EMBC44109.2020.9176476.

[16] R. Jafary, S. Armstrong, T. Byrne, A. Stephens, V. Pellegrino, and S. D. Gregory, 'Fabrication and characterization of tissue-mimicking phantoms for ultrasound-guided cannulation training', *ASAIO Journal*, vol. 68, no. 7, p. 940, Jul. 2022, doi: 10.1097/MAT.0000000000001593.

[17] 'UV-Vis spectrum of methylene blue solution, with maximu | Open-i'. https://openi.nlm.nih.gov/detailedresult?img=PMC2808005_ijms-10-04707f6&req=4 (accessed Mar. 02, 2023).

[18] K. Budidha, V. Rybynok, and P. A. Kyriacou, 'Design and development of a modular, multichannel photoplethysmography system', *IEEE Transactions on Instrumentation and Measurement*, vol. 67, no. 8, pp. 1954–1965, Aug. 2018, doi: 10.1109/TIM.2018.2810643.

[19] G. Bradley, 'PPGExtract'. Feb. 26, 2023. Accessed: Mar. 01, 2023. [Online]. Available: https://github.com/Enantiodromis/PPGExtract